Electronic Supplementary Information

Synthesis of new allyl palladium complexes bearing purine-based NHC ligands with antiproliferative and proapoptotic activity on human ovarian cancer cell lines

Thomas Scattolin[a], Isabella Caligiuri[b], Luciano Canovese[a], Nicola Demitri[c], Roberto Gambari[d], Ilaria Lampronti[d], Flavio Rizzolio[a,b], Claudio Santo[a] and Fabiano Visentin*[a]

[a]Dipartimento di Scienze Molecolari e Nanosistemi, Università Ca' Foscari, Campus Scientifico Via Torino 155, 30174 Venezia-Mestre, Italy. E-mail: fvise@unive.ita;
[b] Pathology Unit, Department of Molecular Biology and Translational Research, National Cancer Institute and Center for Molecular Biomedicine - CRO, Aviano, Italy.
[c]Elettra – Sincrotrone Trieste, S.S. 14 Km 163.5 in Area Science Park, 34149 Basovizza, Trieste, Italy,
[d]Dipartimento di Scienze della Vita e Biotecnologie, Università degli Studi di Ferrara, Via Fossato di Mortara 74, 44121 Ferrara, Italy.

CONTENTS

- **Figure S8 :** $^{13}C\{H^1\}$ NMR spectrum of complex **4a** in $CDCl_3$ at 298K.
- **Figure S9 :** HMQC spectrum of complex **4a** in $CDCl_3$ at 298K.
- **Figure S10 :** ^1H NMR spectrum of complex **4b** in $CDCl_3$ at 298K.
- **Figure S11 :** $^{31}P\{H^1\}$ NMR spectrum of complex **4b** in $CDCl_3$ at 298K.
- **Figure S12 :** ^1H NMR spectrum of complex **5a** in D_2O at 298K.
- **Figure S13 :** $^{31}P\{H^1\}$ NMR spectrum of complex **5a** in D_2O at 298K.
- **Figure S14 :** $^{13}C\{H^1\}$ NMR spectrum of complex **5a** in D_2O at 298K.
- **Figure S15 :** HSQC spectrum of complex **5a** in D_2O at 298K.
- **Figure S16 :** ^1H NMR spectrum of complex **6a** in $CDCl_3$ at 298K.
- **Figure S17 :** $^{13}C\{H^1\}$ NMR spectrum of complex **6a** in $CDCl_3$ at 298K.
- **Figure S18 :** HMQC spectrum of complex **6a** in $CDCl_3$ at 298K.
- **Figure S19 :** IR spectrum of complex **6a** in KBr.
- **Figure S20 :** ^1H NMR spectrum of complex **8a** in CD_3CN at 298K.
- **Figure S21 :** $^{13}C\{H^1\}$ NMR spectrum of complex **8a** in CD_3CN at 298K.
- **Figure S22 :** HMQC spectrum of complex **8a** in CD_3CN at 298K.
- **Table S1.** Effects of the Pd-complexes on the proliferation of MRC-5 cells. The inhibition of cell growth is represented as IC_{50}
- **Figure S23 :** (A-E) Apoptosis profile of A2780 cells untreated (**C-**), treated with cisplatin (**C+**) and with Pd complexes at different concentrations for 72 h.
- **Figure S24 :** (A-E) Apoptosis profile of SKOV-3 cells untreated (**C-**), treated with cisplatin (**C+**) and with Pd complexes at different concentrations for 72 h.
- **Figure S25 :** Ellipsoid representation of **4a** (A) and **8d** (B) crystals ASU contents (50% probability).
- **Figure S26 :** Ortep representations of complexes **4a** (A) and **8d** (B). Atom labels in use are reported.

- **Figure S27 :** Stick representation of overlapped molecular models of **8d** and the related triphenylphosphine-(η^3-allyl)-(tetramethylimidazolin-2-ylidene)-palladium structure (CCDC Number: 714135).
- **Figure S28 :** $^{31}P\{H^1\}$ NMR spectra of complex **4b** in DMSO-d6/D_2O recorded immediately, 24 and 48 hours after the preparation of the solution at T = 298K.
- **Figure S29 :** H^1 NMR spectra of complex **6d** in DMSO-d6/D_2O recorded immediately, 24 and 48 hours after the preparation of the solution at T = 298K.
- **Figure S30 :** H^1 NMR spectra of complex **8a** in DMSO-d6/D_2O recorded immediately, 24 and 48 hours after the preparation of the solution at T = 298K.
- **Table S2:** Crystallographic data of complexes **4a** and **8d**.
- **Table S3 :** Selected bond distances and angles (Å and degrees) for **4a** and **8d** palladium coordination spheres. Naming schemes are reported in Fig.S2.

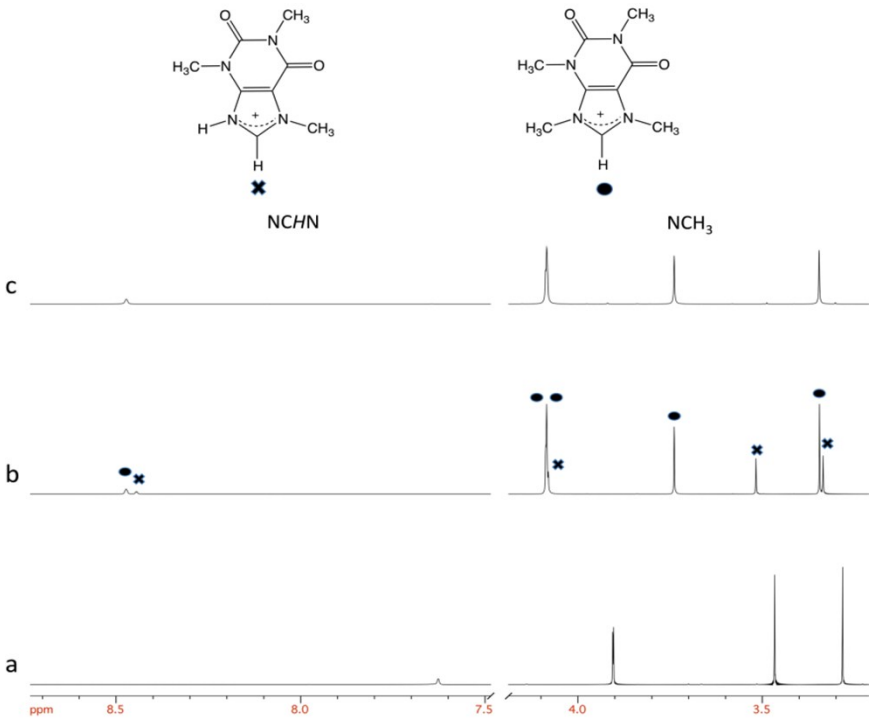

Fig S1: a) Selected portions of the ^{1}H NMR spectrum of the starting caffeine in CD_3CN at RT.

b) Selected portions of the ^{1}H NMR spectrum of the reaction products obtained in the absence of added Na_2CO_3 in CD_3CN at RT.

c) Selected portions of the ^{1}H NMR spectrum of the reaction product **2a** obtained in the presence of added Na_2CO_3 in CD_3CN at RT.

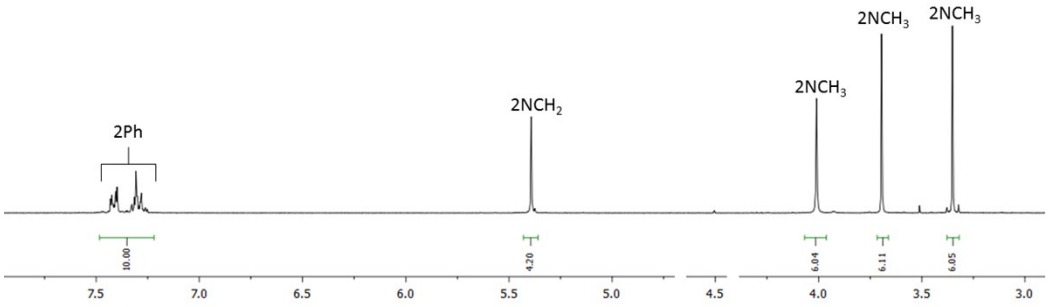

Fig S2: ^{1}H NMR spectrum of 1:1 mixture of **3c** and $AgBF_4$

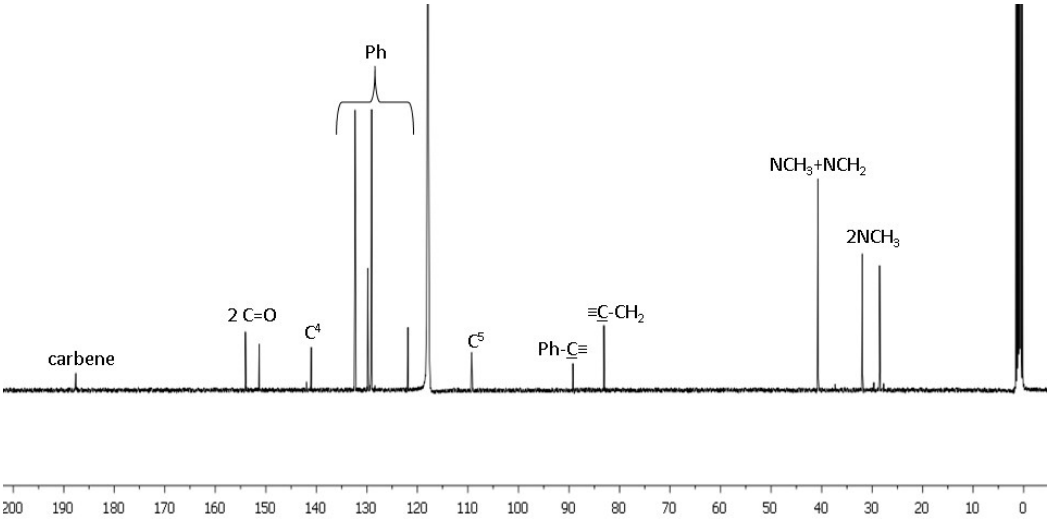

Fig S3: $^{13}C\{H^{1}\}$ NMR spectrum of 1:1 mixture of **3c** and $AgBF_4$

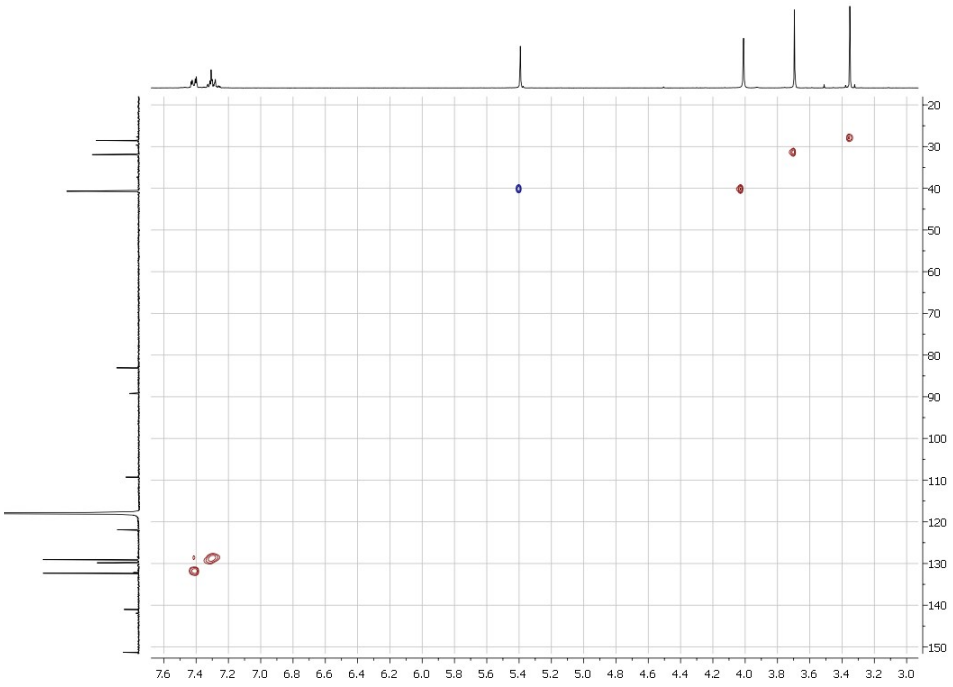

Fig S4: HSQC spectrum of 1:1 mixture of **3c** and $AgBF_4$

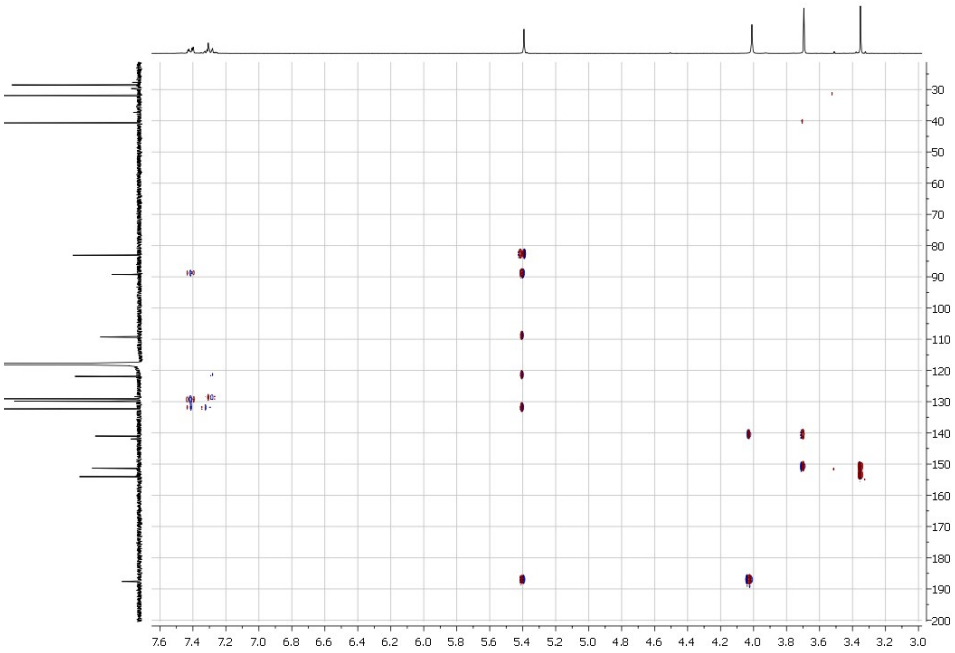

Fig S5: HMBC spectrum of 1:1 mixture of **3c** and $AgBF_4$

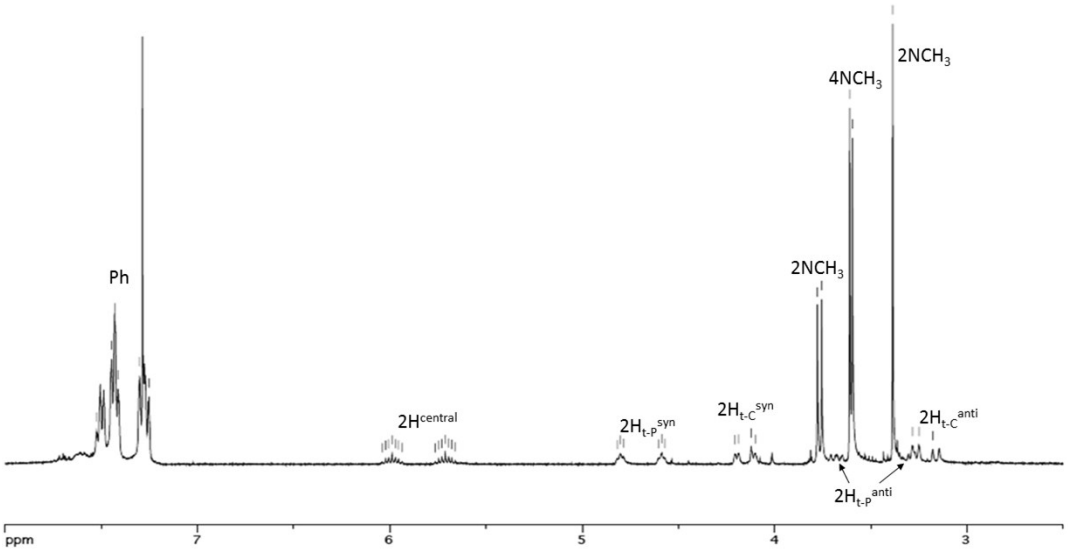

Fig S6: ^{1}H NMR spectrum of complex **4a** in $CDCl_3$ at 298K.

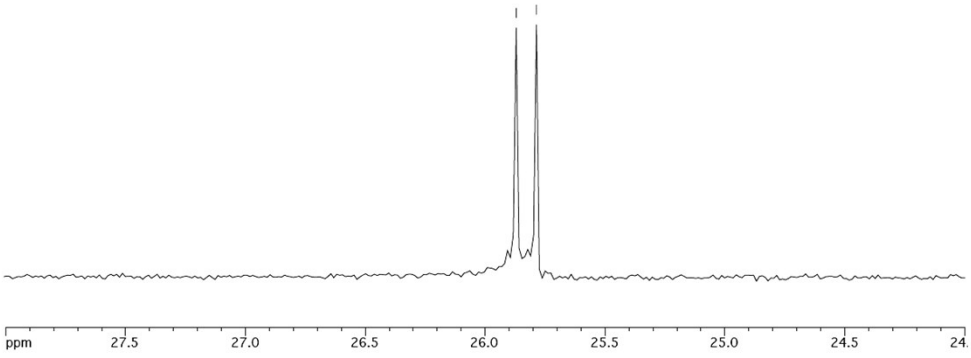

Fig S7: $^{31}P\{H^{1}\}$ NMR spectrum of complex **4a** in $CDCl_3$ at 298K.

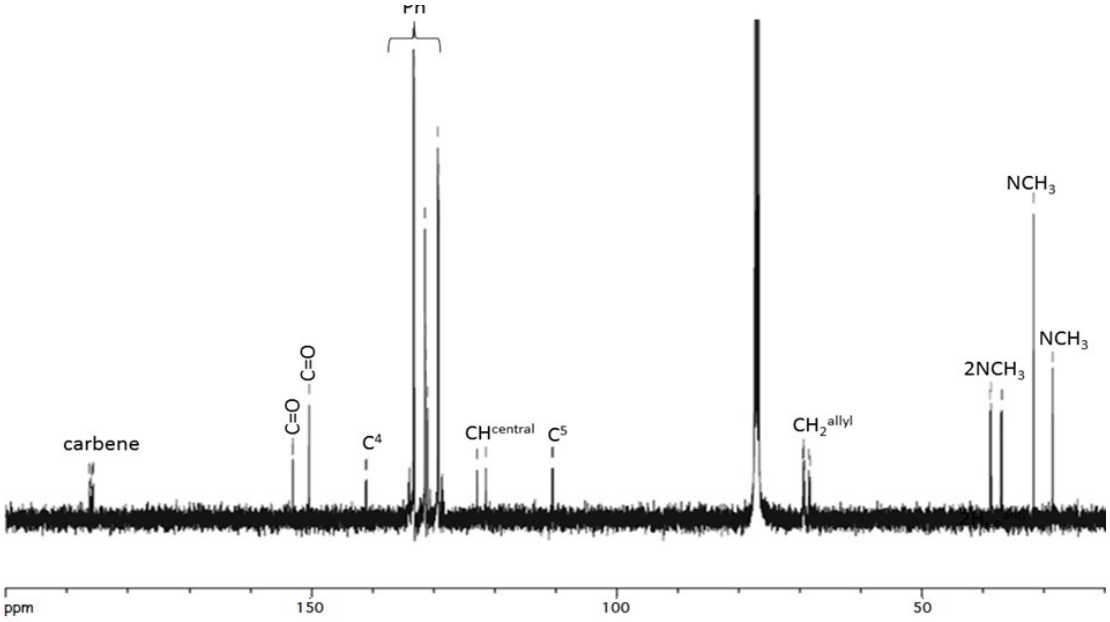

Fig S8: $^{13}C\{H^1\}$ NMR spectrum of complex **4a** in $CDCl_3$ at 298K.

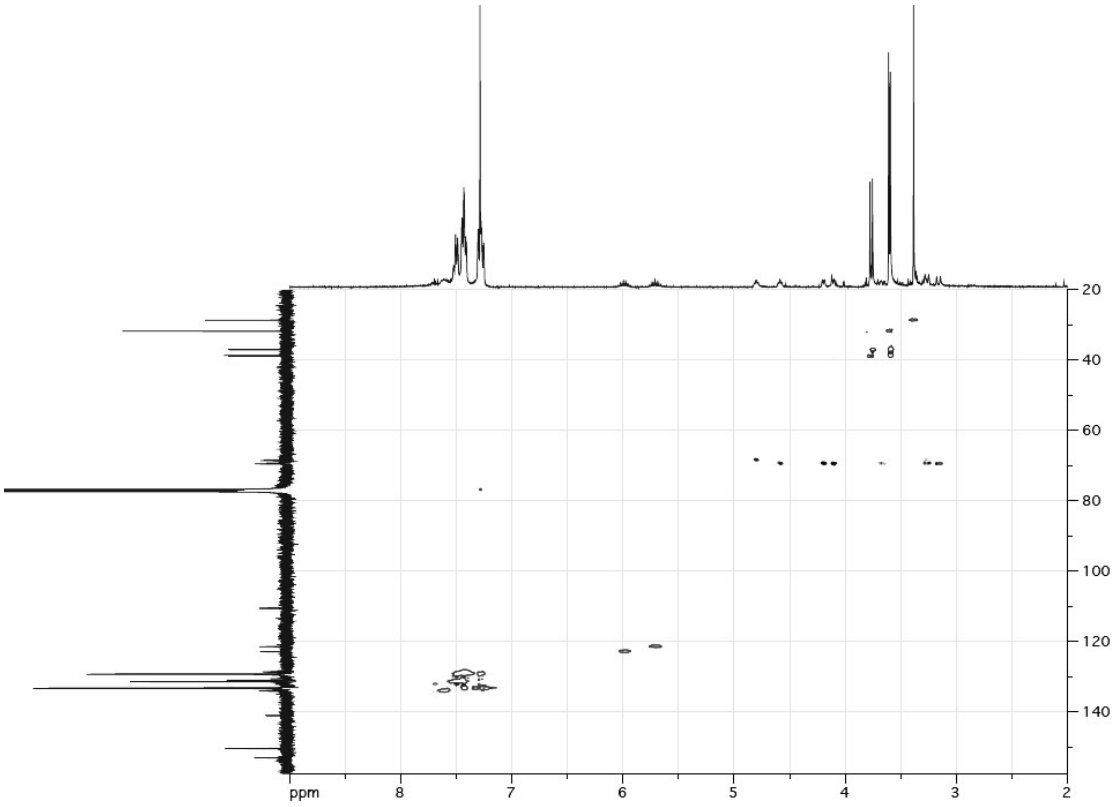

Fig S9: HMQC spectrum of complex **4a** in $CDCl_3$ at 298K.

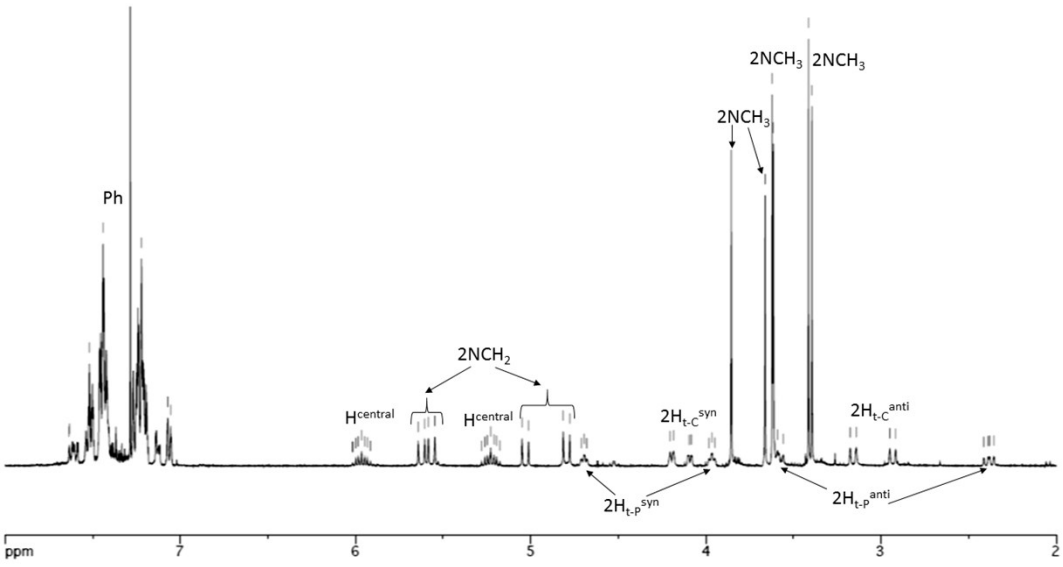

Fig S10: ^{1}H NMR spectrum of complex **4b** in $CDCl_3$ at 298K.

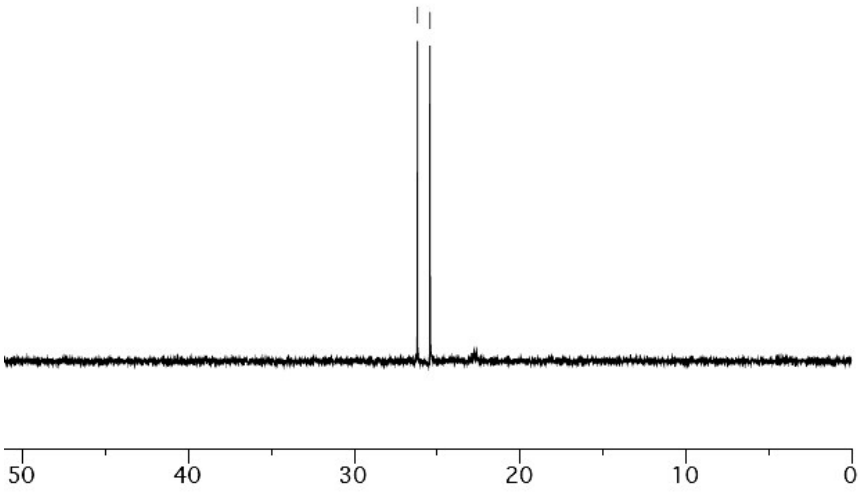

Fig S11: $^{31}P\{H^{1}\}$ NMR spectrum of complex **4b** in $CDCl_3$ at 298K.

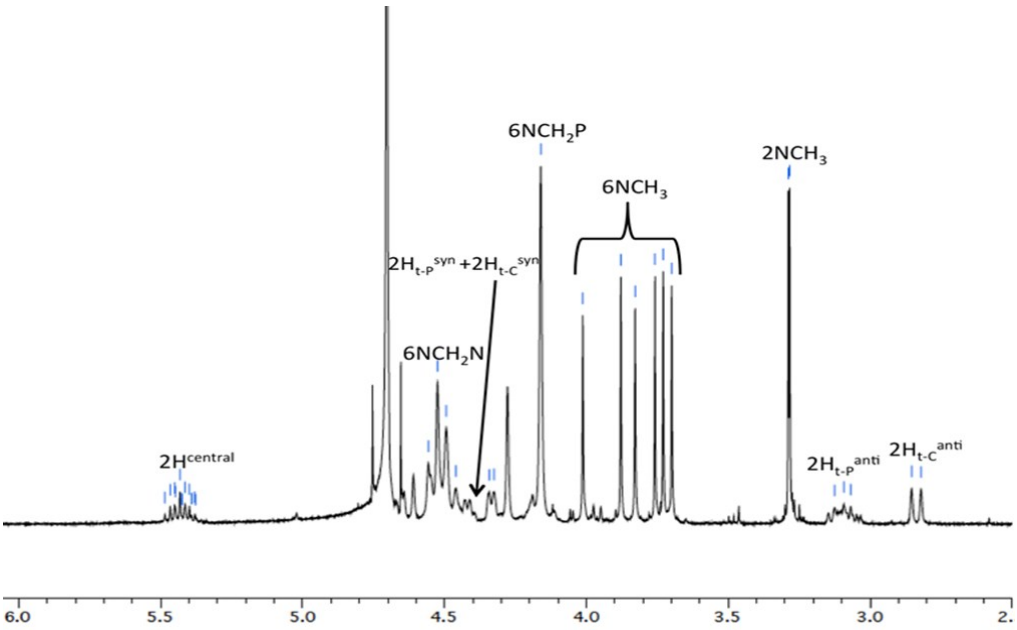

Fig S12: ^{1}H NMR spectrum of complex **5a** in D_2O at 298K.

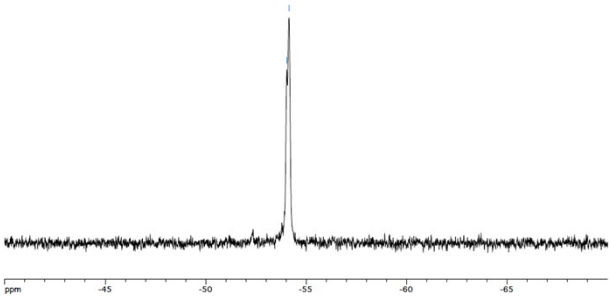

Fig S13: $^{31}P\{H^{1}\}$ NMR spectrum of complex **5a** in D_2O at 298K.

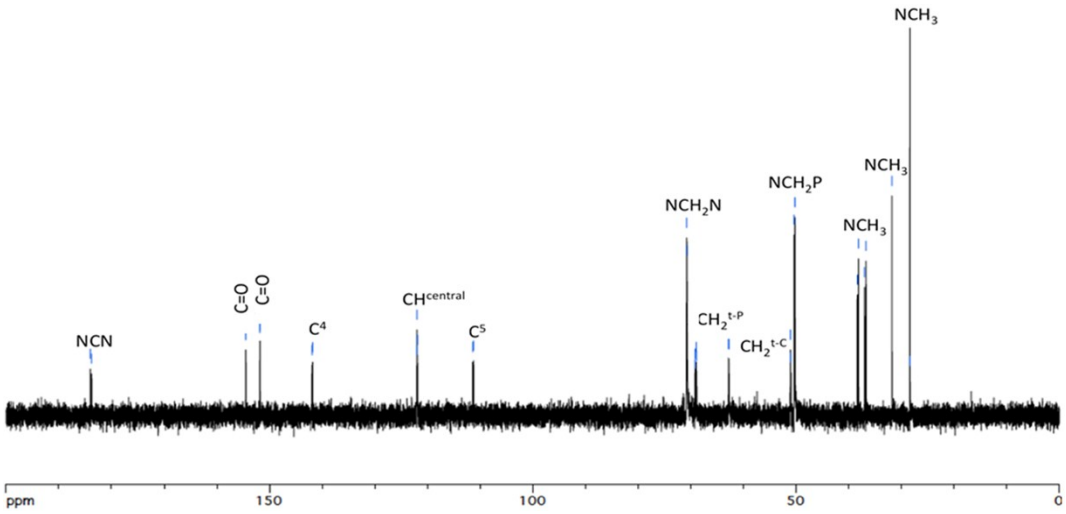

Fig S14: $^{13}C\{H^1\}$ NMR spectrum of complex **5a** in D_2O at 298K.

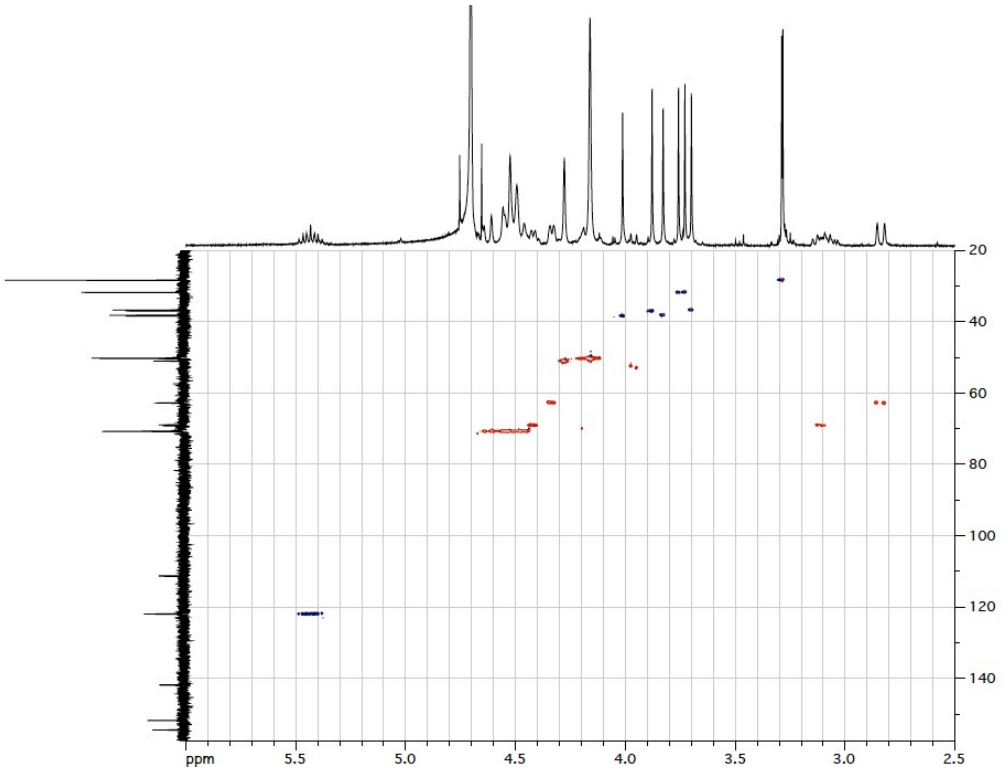

Fig S15: HSQC spectrum of complex **5a** in D_2O at 298K.

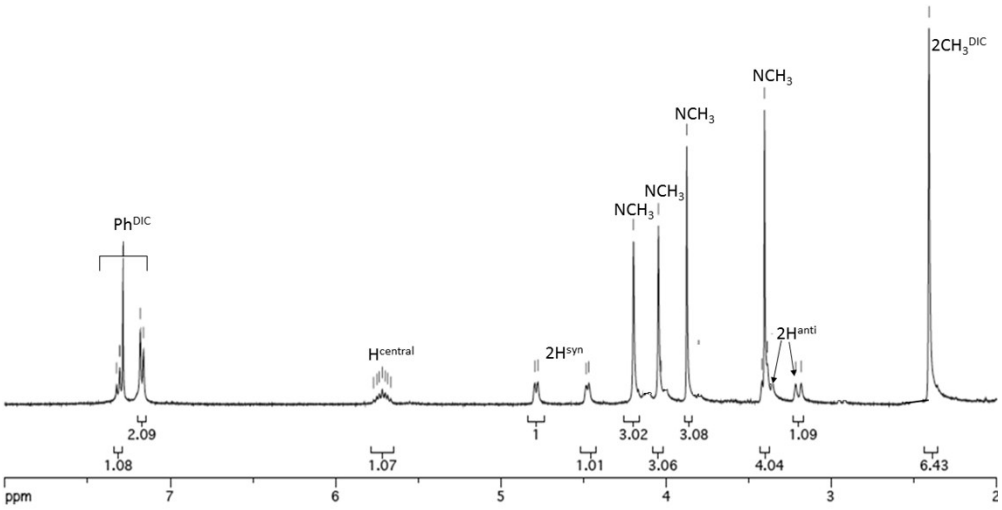

Fig S16: ^{1}H NMR spectrum of complex **6a** in $CDCl_3$ at 298K.

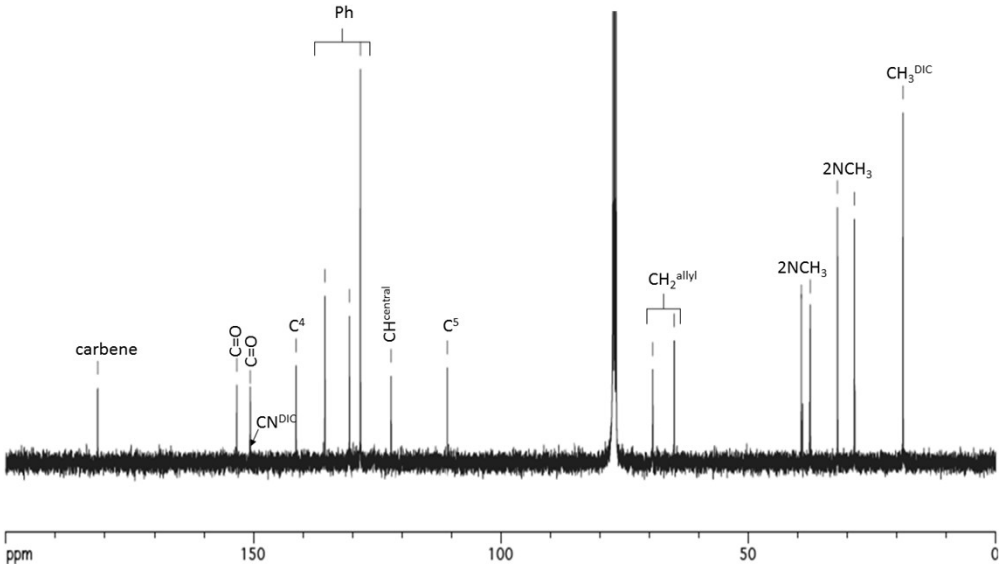

Fig S17: $^{13}C\{H^1\}$ NMR spectrum of complex **6a** in $CDCl_3$ at 298K.

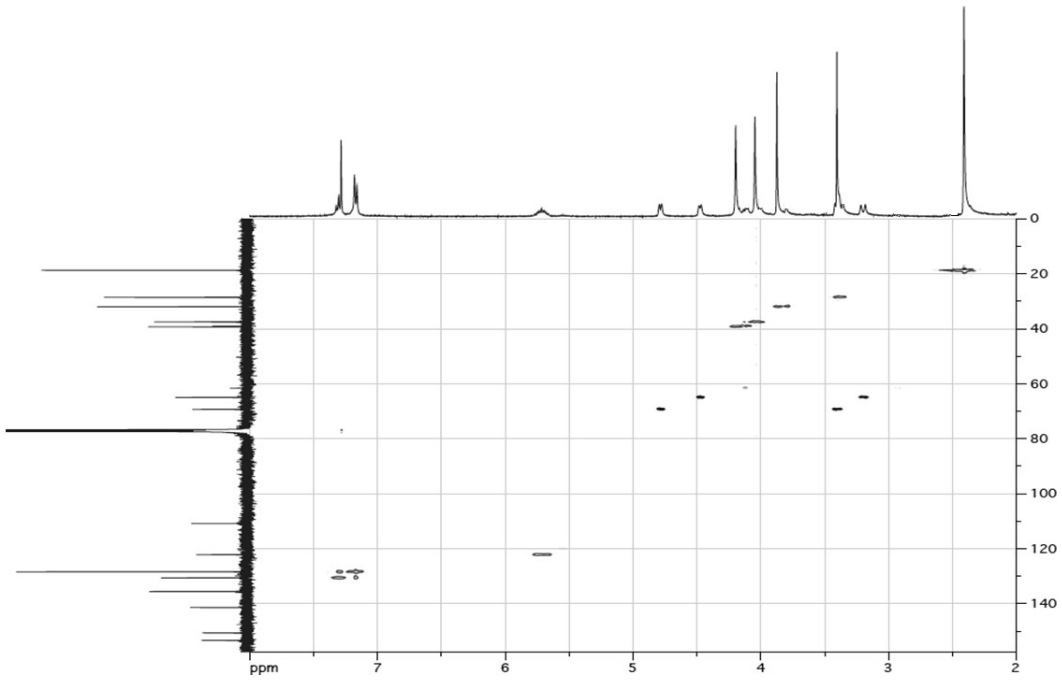

Fig S18: HMQC spectrum of complex **6a** in $CDCl_3$ at 298K.

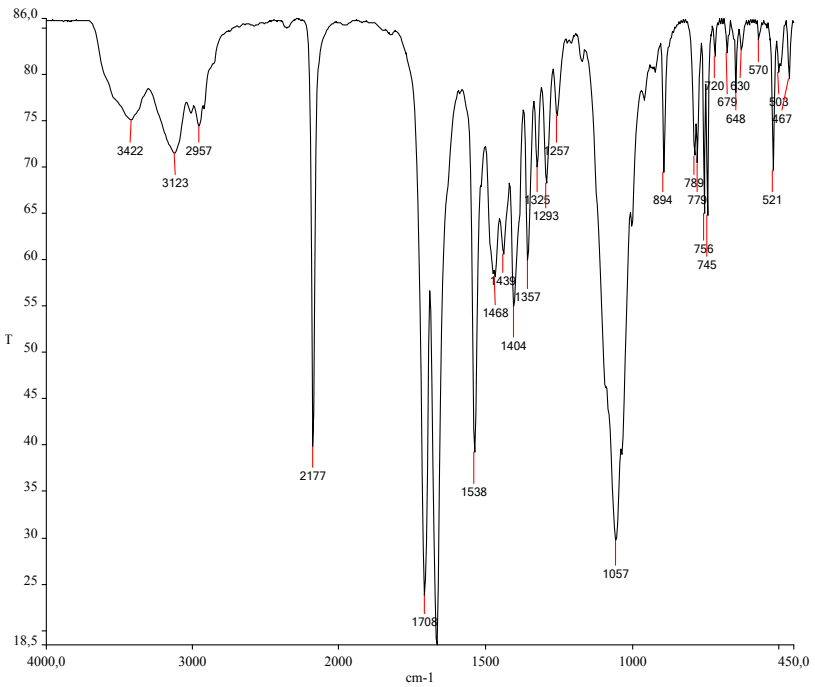

Fig S19: IR spectrum of complex **6a** in KBr

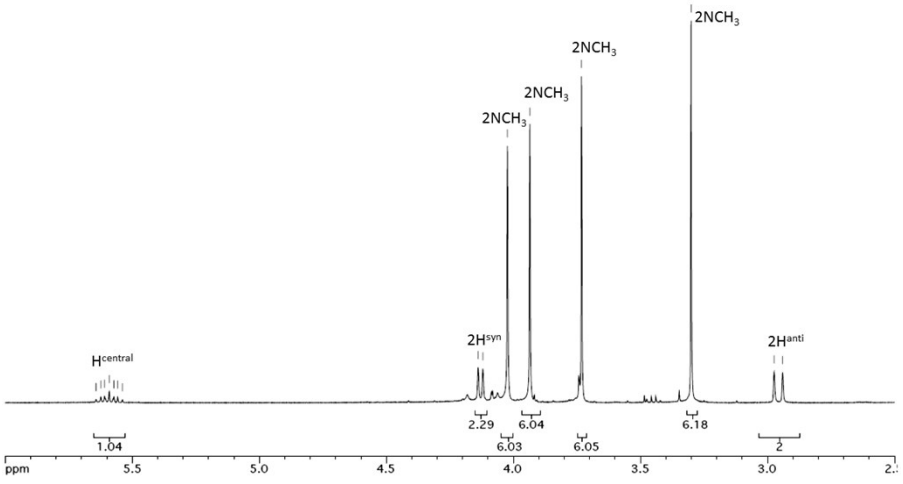

Fig S20: ^{1}H NMR spectrum of complex **8a** in CD_3CN at 298K.

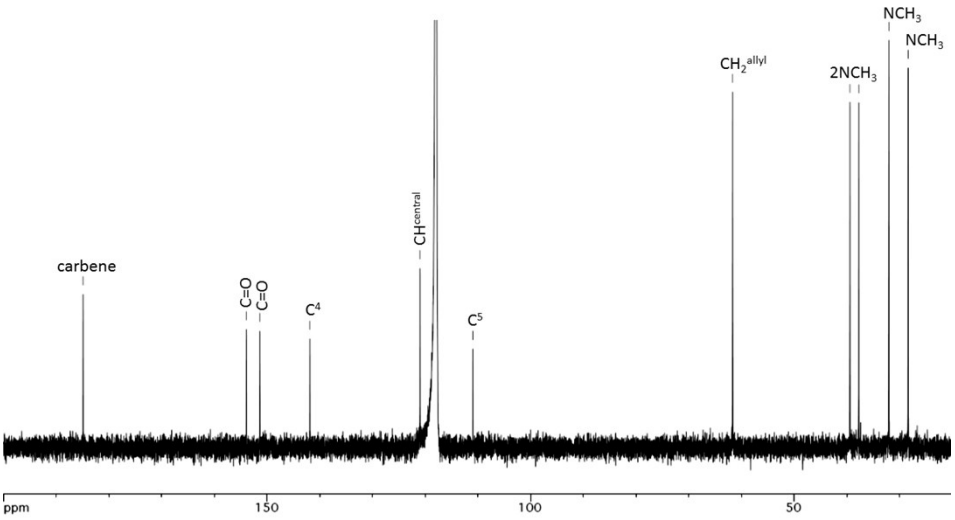

Fig S21: $^{13}C\{H^1\}$ NMR spectra of complex **8a** in CD_3CN at 298K.

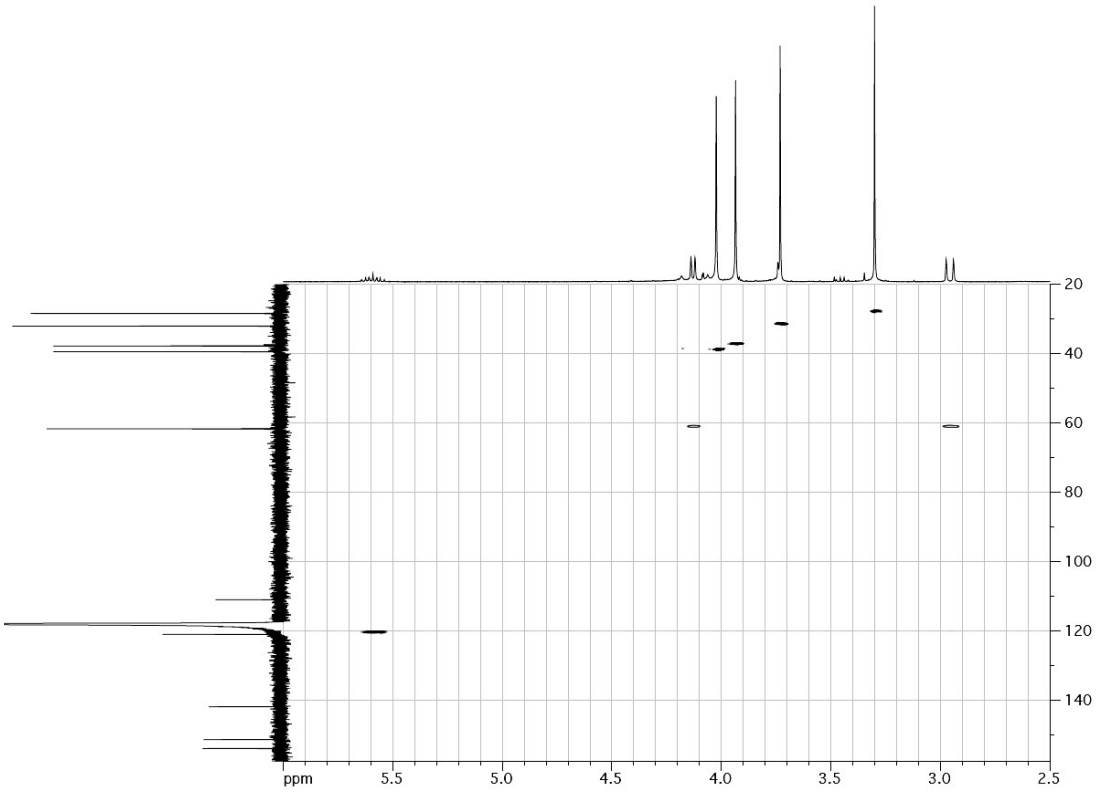

Fig S22: HMQC spectra of complex **8a** in CD_3CN at 298K.

Complex	**MRC-5 (IC_{50})**
Cisplatin	14 ± 1
4d	> 100
5d	22 ± 6
6b	17 ± 1
8a	> 100

Table S1. Effects of the Pd-complexes on the proliferation of MRC-5 cells. The inhibition of cell growth is represented as IC_{50}.

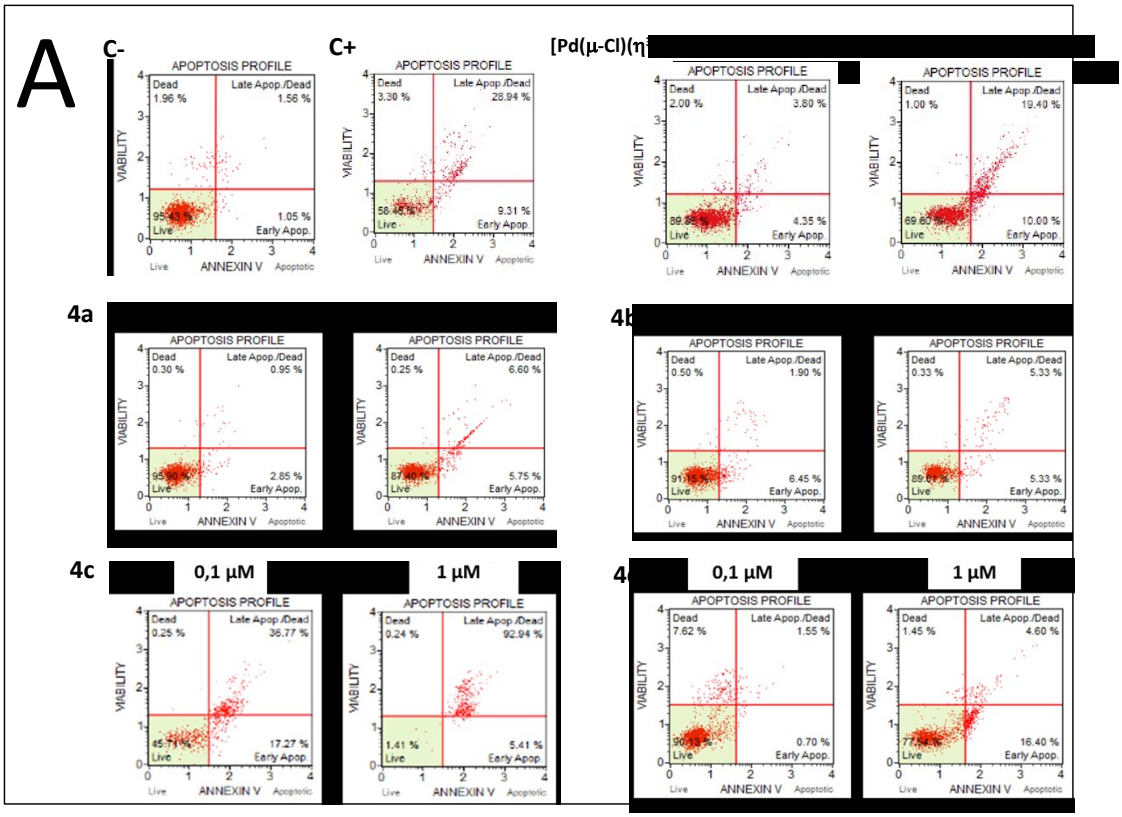
A
C-
C+
[Pd(μ-Cl)(η
4a
4b
4c
0,1 μM
1 μM
APOPTOSIS PROFILE
Dead
Late Apop./Dead
Live
Early Apop.
VIABILITY
ANNEXIN V
Apoptotic

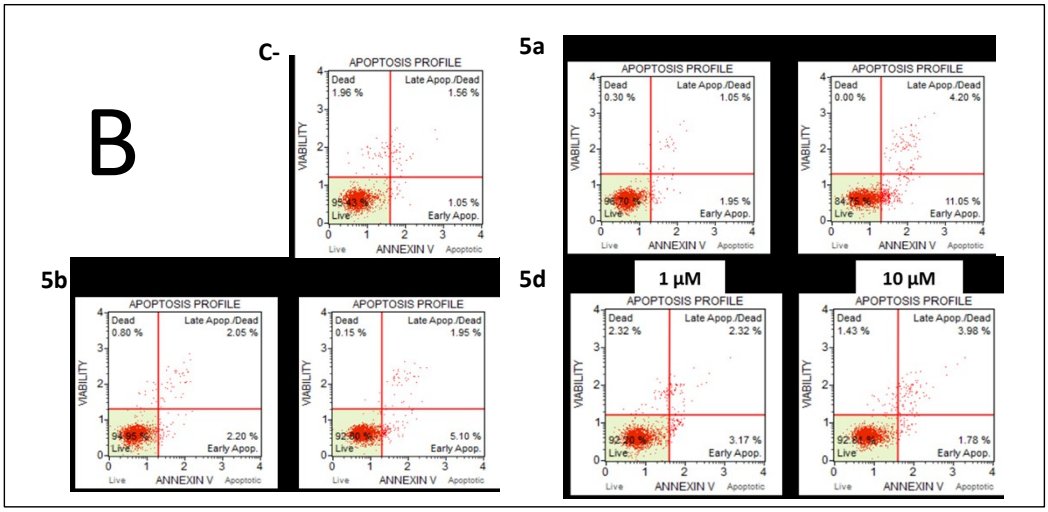
B
C-
5a
5b
5d
1 μM
10 μM
APOPTOSIS PROFILE
Dead
Late Apop./Dead
Live
Early Apop.
VIABILITY
ANNEXIN V
Apoptotic

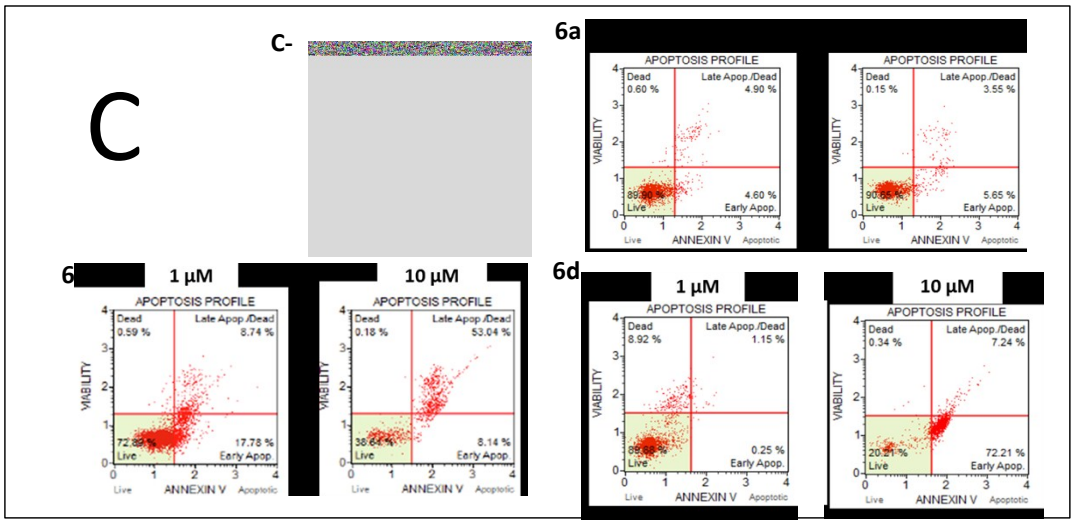
C
C-
6a
APOPTOSIS PROFILE
Dead
0.60 %
Late Apop./Dead
4.90 %
4.60 %
Early Apop.
Live
ANNEXIN V
Apoptotic
VIABILITY
Dead
0.15 %
Late Apop./Dead
3.55 %
5.65 %
Early Apop.
6
1 µM
10 µM
Dead
0.59 %
Late Apop./Dead
8.74 %
17.78 %
Dead
0.18 %
Late Apop./Dead
53.04 %
8.14 %
6d
1 µM
10 µM
Dead
8.92 %
Late Apop./Dead
1.15 %
0.25 %
Dead
0.34 %
Late Apop./Dead
7.24 %
72.21 %

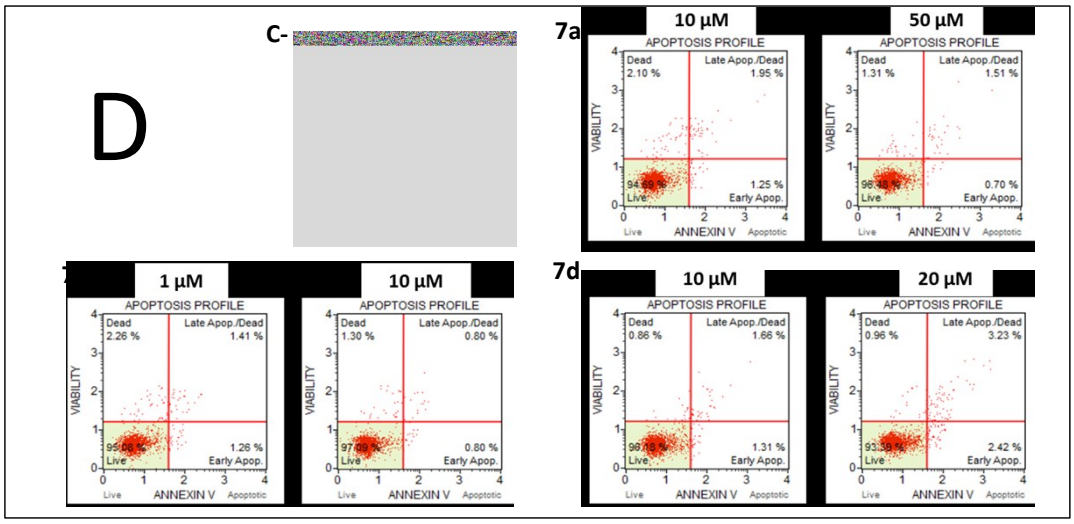
D
C-
7a
10 µM
50 µM
APOPTOSIS PROFILE
Dead
2.10 %
Late Apop./Dead
1.95 %
1.25 %
Early Apop.
Live
ANNEXIN V
Apoptotic
VIABILITY
Dead
1.31 %
Late Apop./Dead
1.51 %
0.70 %
7
1 µM
10 µM
Dead
2.26 %
Late Apop./Dead
1.41 %
1.26 %
Dead
1.30 %
Late Apop./Dead
0.80 %
0.80 %
7d
10 µM
20 µM
Dead
0.86 %
Late Apop./Dead
1.66 %
1.31 %
Dead
0.96 %
Late Apop./Dead
3.23 %
2.42 %

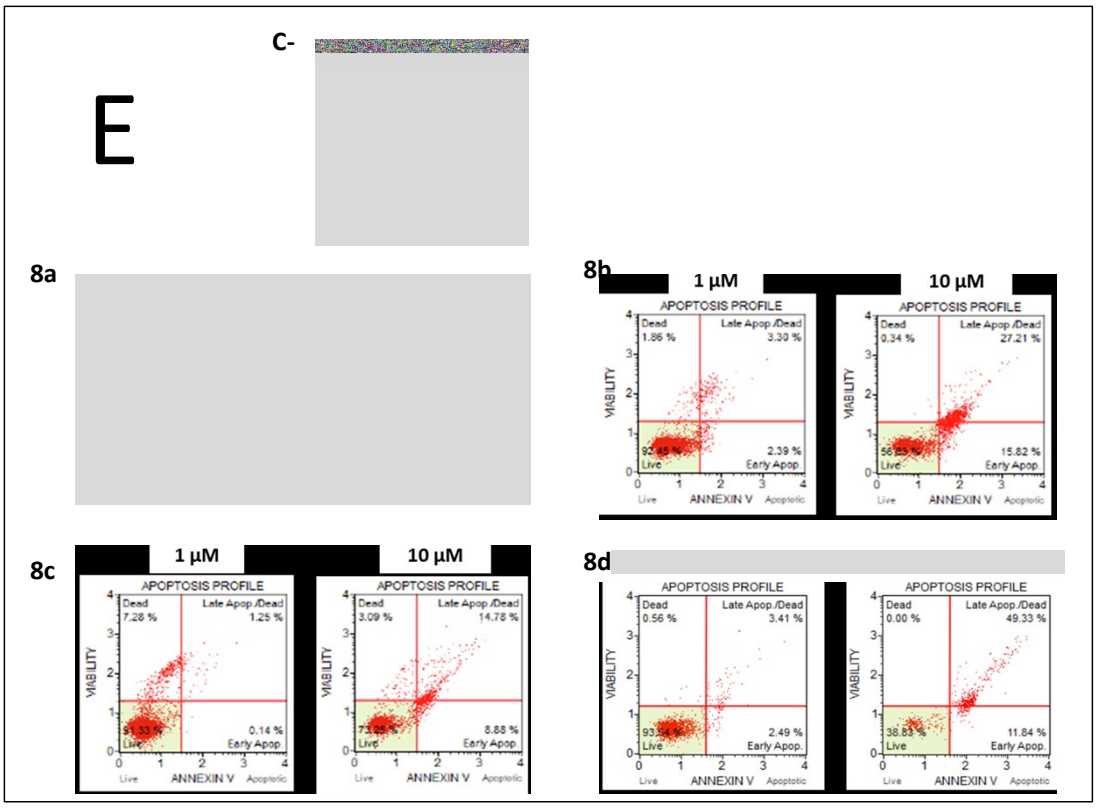

Fig. S23: (A-E) Apoptosis profile of A2780 cells untreated (**C-**), treated with cisplatin (**C+**), and with Pd complexes at different concentrations for 72 h.

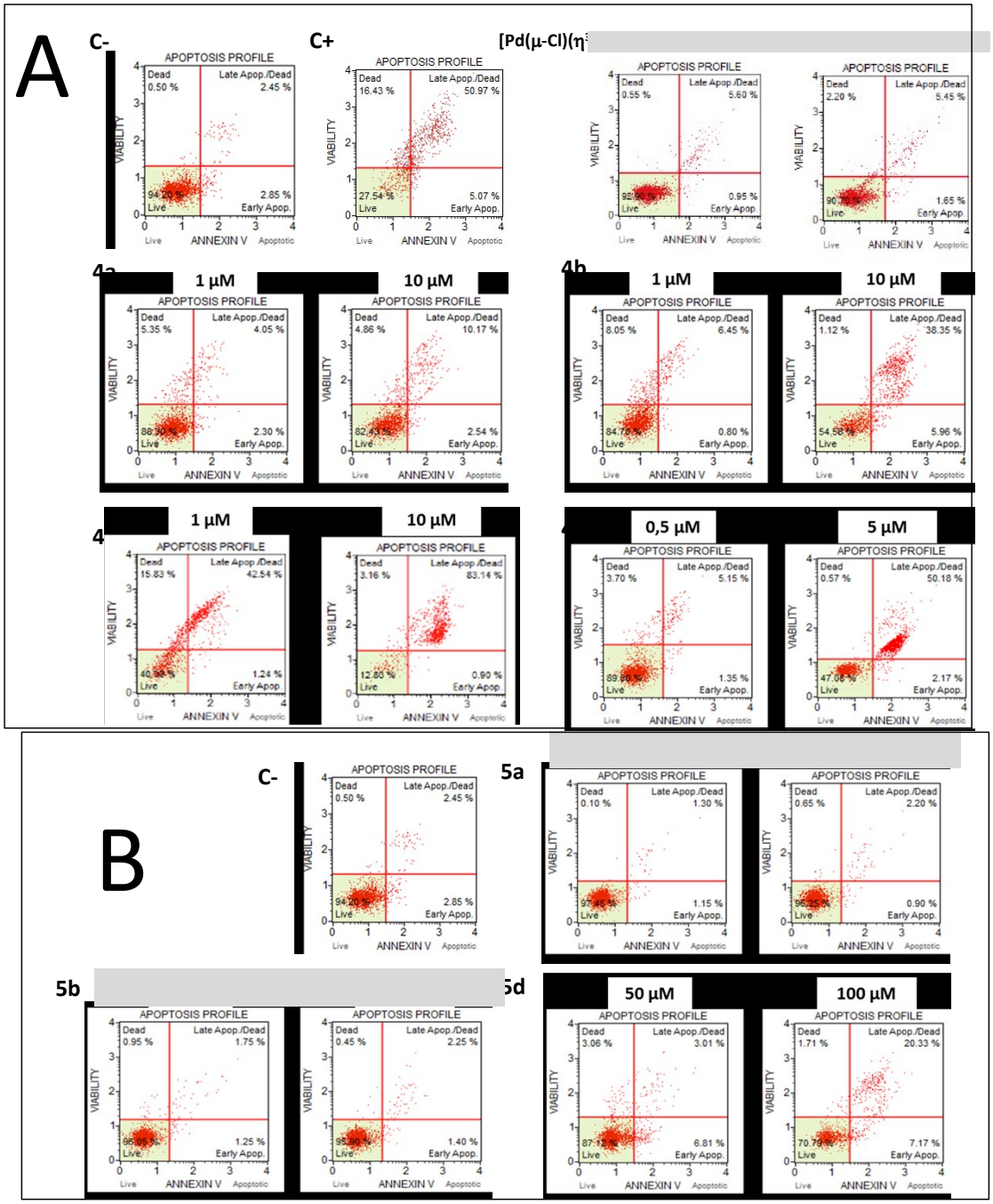
A
C-
C+
[Pd(μ-Cl)(η
4a
1 μM
10 μM
4b
1 μM
10 μM
4
1 μM
10 μM
0,5 μM
5 μM
B
C-
5a
5b
5d
50 μM
100 μM
APOPTOSIS PROFILE
VIABILITY
ANNEXIN V
Live
Apoptotic
Dead
Late Apop./Dead
Early Apop.

C

C-

6a

6

6d

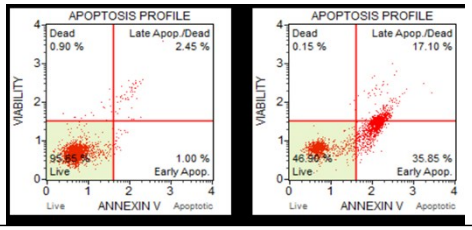

D

C-

7a

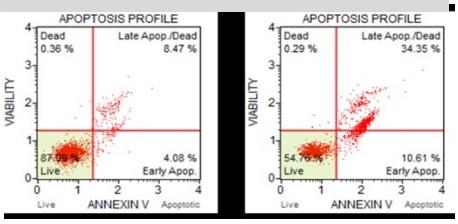

25 µM

50 µM

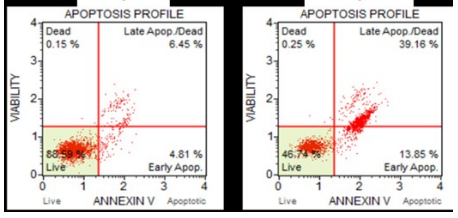

7d

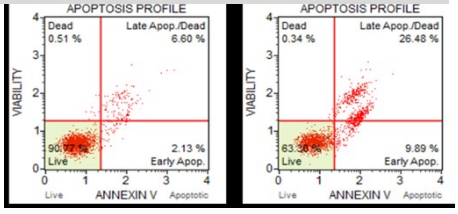

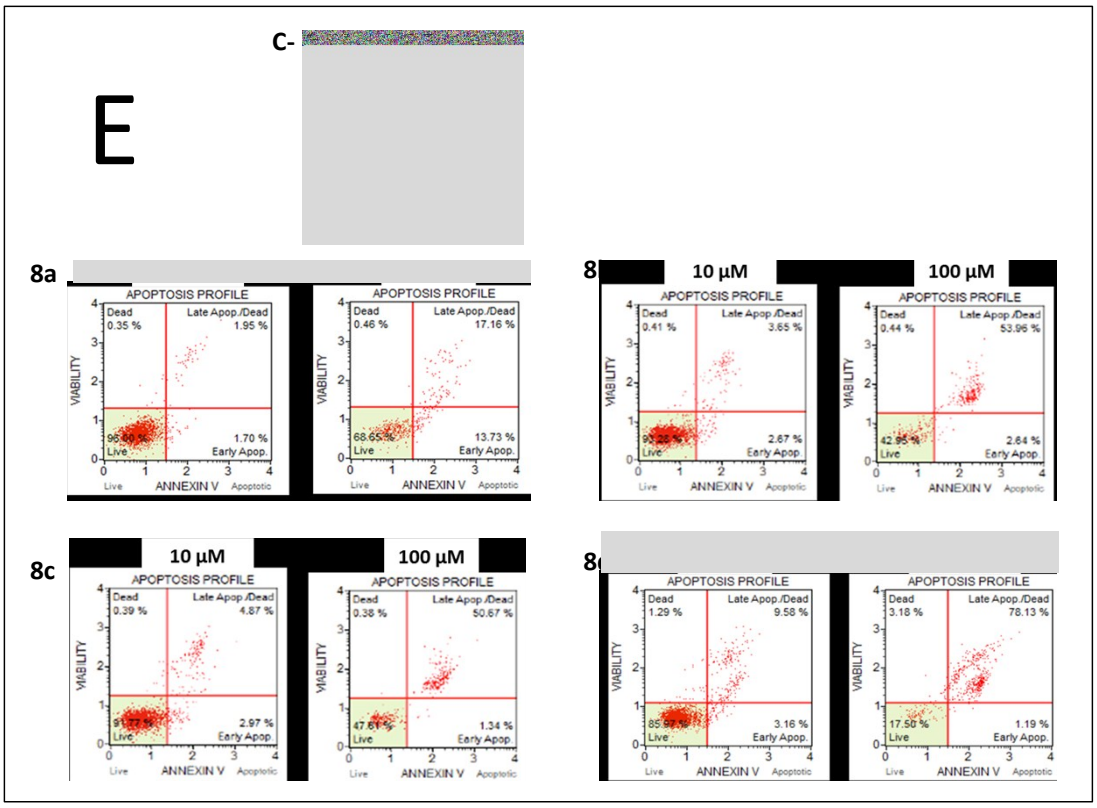

Fig. S24: (A-E) Apoptosis profile of SKOV-3 cells untreated (**C-**), treated with cisplatin (**C+**), and with Pd complexes at different concentrations for 72 h.

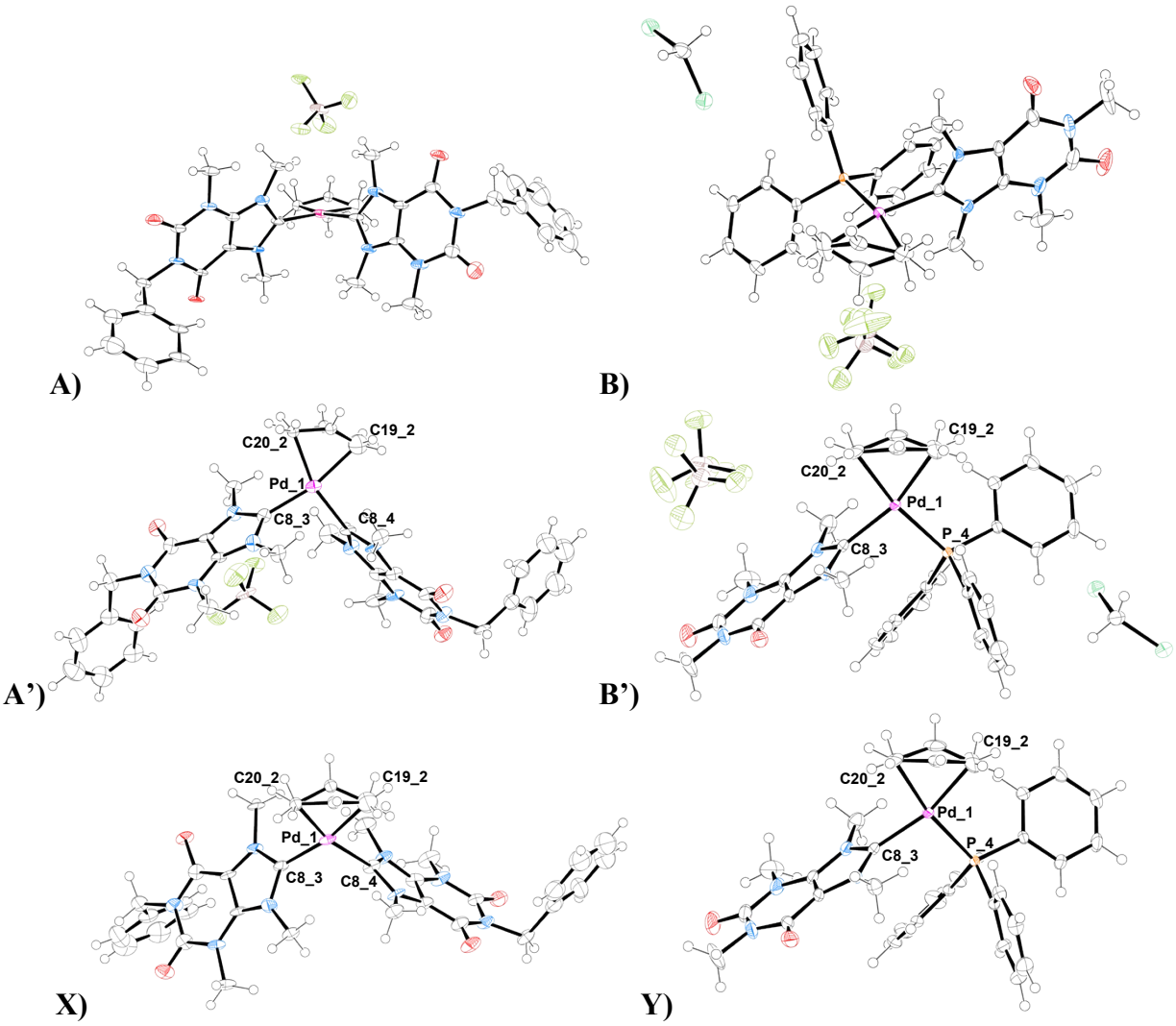

Figure S25. Ellipsoid representation of **8d** (A) and **4a** (B) crystals ASU contents (50% probability).

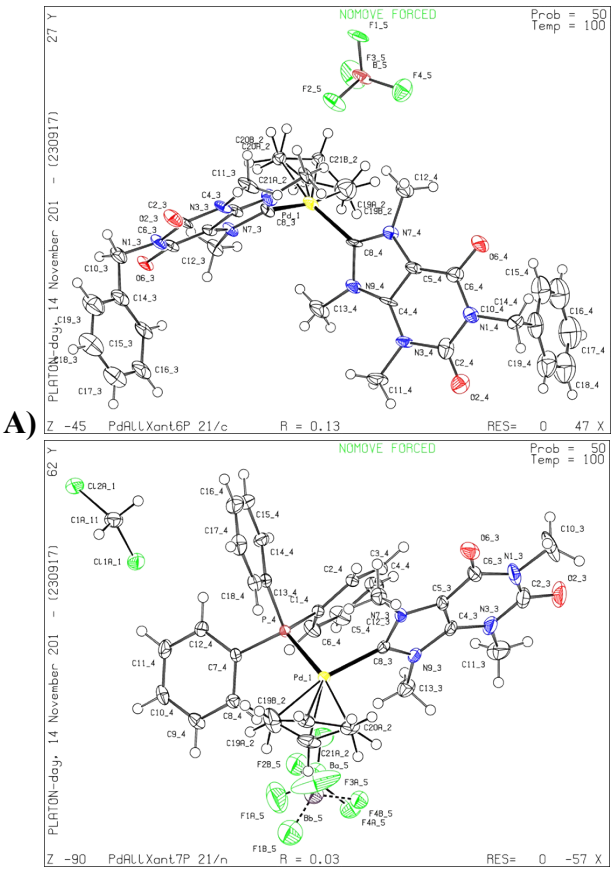

Figure S26. Ortep representations of complexes **8d** (A) and **4a**(B). Atom labels in use are reported.

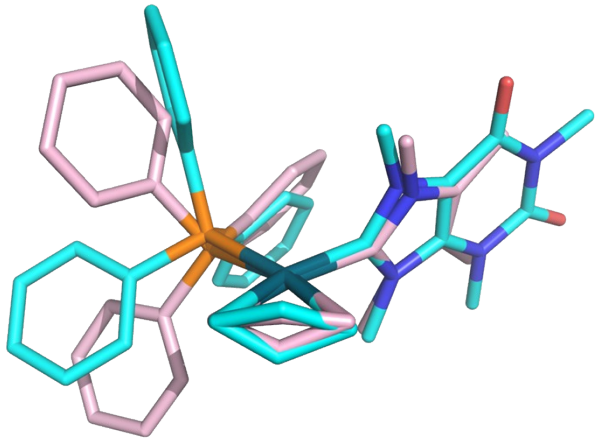

Figure S27. Stick representation of overlapped molecular models of **4a** (blue sticks) and the related triphenylphosphine-(η3-allyl)-(tetramethylimidazolin-2-ylidene)-palladium structure (pink sticks - CCDC Number: 714135).

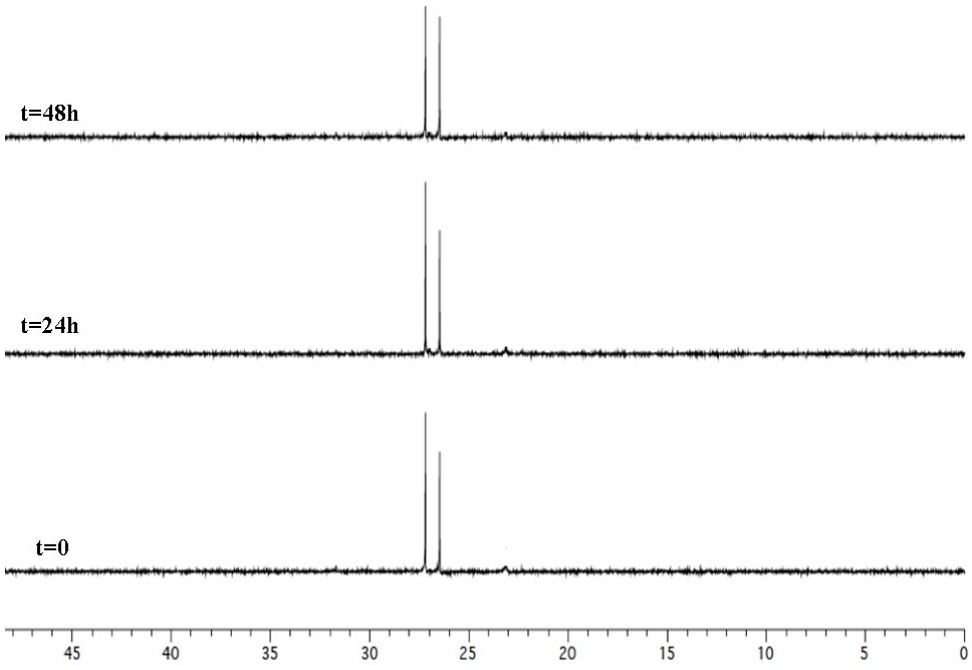

Figure S28. $^{31}P\{H^1\}$ NMR spectra of complex **4b** in DMSO-d6/D_2O recorded immediately, 24 and 48 hours after the preparation of the solution at T = 298K.

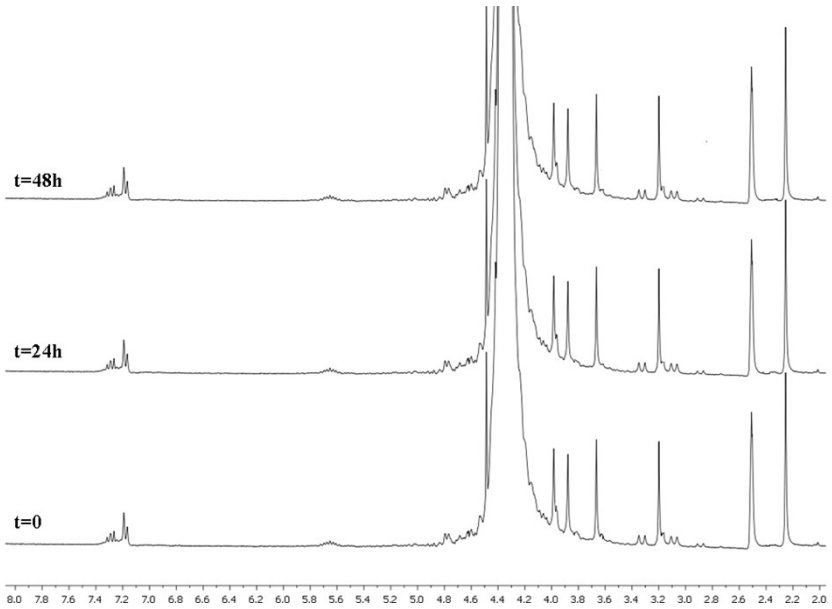

Figure S29. H^1 NMR spectra of complex **6d** in DMSO-d6/D_2O recorded immediately, 24 and 48 hours after the preparation of the solution at T = 298K.

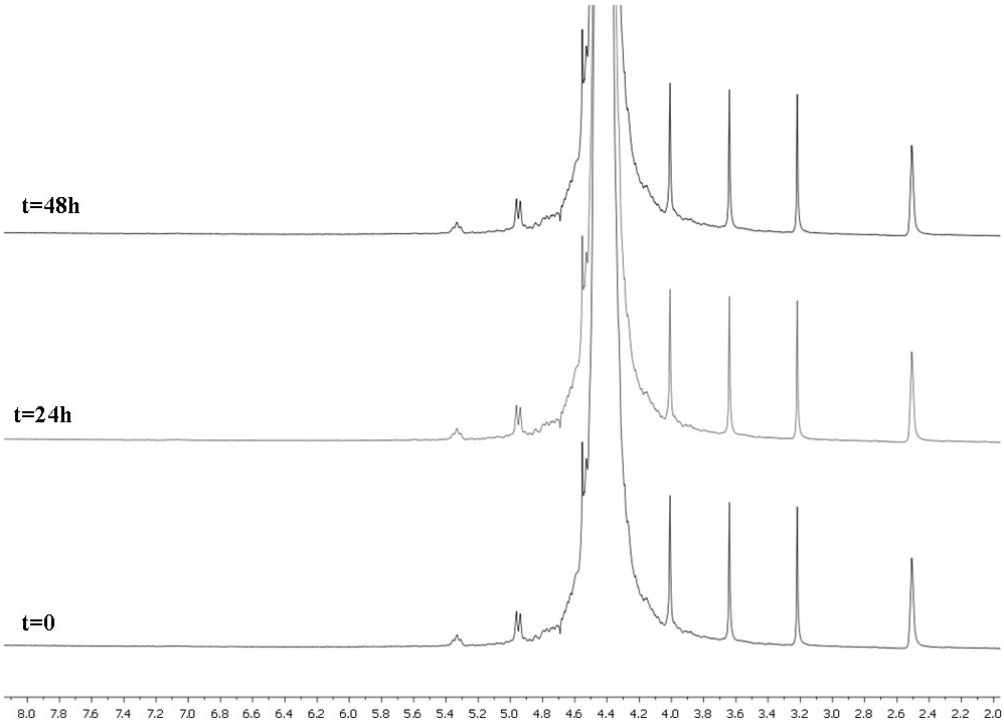

Figure S30. H^1 NMR spectra of complex **8a** in DMSO-d6/D_2O recorded immediately, 24 and 48 hours after the preparation of the solution at T = 298K.

Table S2. Crystallographic data.

Compound	**8d**	**4a**
Formula	$PdC_{33}H_{37}N_8O_4 \cdot BF_4$	$PdC_{30}H_{32}N_4O_2P \cdot BF_4 \cdot 0.5CH_2Cl_2$
M	802.91	747.24
Space group	$P2_1/c$	$P2_1/n$
Crystal system	Monoclinic	Monoclinic
a/Å	8.200(2)	8.818(2)
b/Å	13.605(3)	15.614(3)
c/Å	30.666(6)	23.329(5)
β/°	96.85(3)	94.90(3)
V/Å^3	3396.7(12)	3200.3(11)
Z	4	4
T/K	100	100
D_c/g cm^{-3}	1.570	1.551
F(000)	1640	1516
μ(0.7Å)/cm^{-1}	5.88	7.31
Measured Reflections	77120	38281
Unique Reflections	6783	8782
R_{int}	0.0311	0.0304
Obs. Refl.ns [I≥2σ(I)]	6042	8453
θ_{min}- θ_{max}/°	1.32 – 25.77	1.55 – 29.08
hkl ranges	-10,10; -16,16; -14,38	-11,11; -21,21; -32,32
R(F^2) (Obs.Refl.ns)	0.1325	0.0276
wR(F^2) (All Refl.ns)	0.3219	0.0714
No. Variables	407	449
Goodness of fit	1.139	1.000
$\Delta\rho_{max}$; $\Delta\rho_{min}$ /e Å^{-3}	3.95; -4.43	1.20; -0.90
CCDC Deposition N.	1825947	1825948

Table S3. Selected bond distances and angles (Å and degrees) for **8d** and **4a** palladium coordination spheres. Naming schemes are reported in Fig.S2.

8d				**4a**			
Distances (Å)		**Angles**	**(°)**	**Distances (Å)**		**Angles**	**(°)**
Pd_1-C19_2	2.1653(184)	C19_2-Pd_1-C20_2	68.64(58)	Pd_1-C19_2	2.1776(20)	C19_2-Pd_1-C20_2	67.50(8)
Pd_1-C20_2	2.1467(125)	C8_3-Pd_1-C8_4	98.14(51)	Pd_1-C20_2	2.1543(16)	P_4-Pd_1-C8_3	95.17(4)
Pd_1-C8_3	2. 0298(123)	C8_3-Pd_1-C20_2	98.97(47)	Pd_1-C8_3	2.0354(15)	C8_3-Pd_1-C20_2	94.62(7)
Pd_1-C8_4	2. 0294(120)	C8_4-Pd_1-C19_2	94.38(58)	Pd_1-P_4	2.3041(6)	P_4-Pd_1-C19_2	102.80(6)